

Quasifree (p , $2p$) Reactions on Oxygen Isotopes: Observation of Isospin Independence of the Reduced Single-Particle Strength

L. Atar,^{1,2*} S. Paschalis,^{3,1} C. Barbieri,⁴ C. A. Bertulani,⁵ P. Díaz Fernández,⁶ M. Holl,¹ M. A. Najafi,⁷ V. Panin,^{1,8} H. Alvarez-Pol,⁶ T. Aumann,^{1,2,†} V. Avdeichikov,⁹ S. Beceiro-Novo,⁶ D. Bemmerer,¹⁰ J. Benlliure,⁶ J. M. Boillos,^{6,2} K. Boretzky,² M. J. G. Borge,¹¹ M. Caamaño,⁶ C. Caesar,^{2,1} E. Casarejos,¹² W. Catford,⁴ J. Cederkall,⁹ M. Chartier,¹³ L. Chulkov,¹⁴ D. Cortina-Gil,⁶ E. Cravo,¹⁵ R. Crespo,¹⁶ I. Dillmann,^{17,2} Z. Elekes,¹⁸ J. Enders,¹ O. Ershova,² A. Estrade,¹⁹ F. Farinon,¹ L. M. Fraile,²⁰ M. Freer,²¹ D. Galaviz Redondo,²² H. Geissel,^{2,17} R. Gernhäuser,²³ P. Golubev,⁹ K. Göbel,²⁴ J. Hagdahl,²⁵ T. Heftrich,²⁴ M. Heil,² M. Heine,²⁶ A. Heinz,²⁵ A. Henriques,²² A. Hufnagel,¹ A. Ignatov,¹ H. T. Johansson,²⁵ B. Jonson,²⁵ J. Kahlbow,¹ N. Kalantar-Nayestanaki,⁷ R. Kanungo,²⁷ A. Kelic-Heil,² A. Knyazev,⁹ T. Kröll,¹ N. Kurz,² M. Labiche,²⁸ C. Langer,²⁴ T. Le Bleis,²³ R. Lemmon,²⁸ S. Lindberg,²⁵ J. Machado,²² J. Marganec-Gałązka,^{1,29,2} A. Movsesyan,¹ E. Nacher,¹¹ E. Y. Nikolskii,¹⁴ T. Nilsson,²⁵ C. Nociforo,² A. Perea,¹¹ M. Petri,³ S. Pietri,² R. Plag,² R. Reifarth,²⁴ G. Ribeiro,¹¹ C. Rigollet,⁷ D. M. Rossi,^{1,2} M. Röder,^{10,30} D. Savran,²⁹ H. Scheit,¹ H. Simon,² O. Sorlin,³¹ I. Syndikus,¹ J. T. Taylor,¹³ O. Tengblad,¹¹ R. Thies,²⁵ Y. Togano,⁸ M. Vandebrouck,³¹ P. Velho,²² V. Volkov,¹⁴ A. Wagner,¹⁰ F. Wamers,^{2,1} H. Weick,² C. Wheldon,²¹ G. L. Wilson,³² J. S. Winfield,^{2,17} P. Woods,¹⁹ D. Yakorev,¹⁰ M. Zhukov,²⁵ A. Zilges,³³ and K. Zuber³⁰

(R³B Collaboration)

¹*Institut für Kernphysik, Technische Universität Darmstadt, 64289 Darmstadt, Germany*

²*GSI Helmholtzzentrum für Schwerionenforschung, Planckstraße 1, 64291 Darmstadt, Germany*

³*Department of Physics, University of York, York YO10 5DD, United Kingdom*

⁴*Department of Physics, University of Surrey, Guildford GU2 7XH, United Kingdom*

⁵*Texas A&M University-Commerce, 75428 Commerce, Texas, United States of America*

⁶*Departamento de Física de Partículas, Universidade de Santiago de Compostela, 15706 Santiago de Compostela, Spain*

⁷*KVI-CART, University of Groningen, Zernikelaan 25, 9747 AA Groningen, Netherlands*

⁸*RIKEN, Nishina Center for Accelerator-Based Science, 2-1 Hirosawa, 351-0198 Wako, Saitama, Japan*

⁹*Department of Physics, Lund University, 22100 Lund, Sweden*

¹⁰*Helmholtz-Zentrum Dresden-Rossendorf, Institute of Radiation Physics, P.O.B. 510119, 01314 Dresden, Germany*

¹¹*Instituto de Estructura de la Materia, CSIC, E-28006 Madrid, Spain*

¹²*Universidad de Vigo, 36310 Vigo, Spain*

¹³*University of Liverpool, L69 3BX Liverpool, United Kingdom*

¹⁴*NRC Kurchatov Institute, place Akademika Kurchatova, Moscow 123182, Russia*

¹⁵*Faculdade de Ciências, Universidade de Lisboa, 1749-016 Lisboa, Portugal*

¹⁶*Instituto Superior Técnico, Universidade de Lisboa, 1049-001 Lisboa, Portugal*

¹⁷*Justus-Liebig-Universität Gießen, 35392 Gießen, Germany*

¹⁸*ATOMKI Debrecen, Bem tér 18/c, 4026 Debrecen, Hungary*

¹⁹*University of Edinburgh, EH8 9YL Edinburgh, United Kingdom*

²⁰*Grupo de Física Nuclear & IPARCOS, Universidad Complutense de Madrid, 28040 Madrid, Spain*

²¹*University of Birmingham, B15 2TT Birmingham, United Kingdom*

²²*Nuclear Physics Center, University of Lisbon, 1649-003 Lisboa, Portugal*

²³*Technische Universität München, James-Frank-Strasse 1, 85748 Garching, Germany*

²⁴*Goethe-Universität Frankfurt, Max-von-Laue Straße 1, 60438 Frankfurt am Main, Germany*

²⁵*Chalmers University of Technology, Kemivägen 9, 412 96 Göteborg, Sweden*

²⁶*IPHC-CNRS/Université de Strasbourg, 67037 Strasbourg, France*

²⁷*Saint Mary's University, 923 Robie Street, B3H 3C3 Halifax, Nova Scotia, Canada*

²⁸*Science and Technology Facilities Council—Daresbury Laboratory, WA4 4AD Warrington, United Kingdom*

²⁹*Extreme Matter Institute, GSI Helmholtzzentrum für Schwerionenforschung, Planckstraße 1, 64291 Darmstadt, Germany*

³⁰*Technische Universität Dresden, Institut für Kern- und Teilchenphysik, Zellescher Weg 19, 01069 Dresden, Germany*

³¹*GANIL, Boulevard Henri Becquerel, 14076 Caen, France*

³²University of Surrey, GU2 7XH Surrey, United Kingdom³³Universität zu Köln, Institut für Kernphysik, Zùlpicher Straße 77, 50937 Köln, Germany (Received 14 August 2017; revised manuscript received 8 November 2017; published 29 January 2018)

Quasifree one-proton knockout reactions have been employed in inverse kinematics for a systematic study of the structure of stable and exotic oxygen isotopes at the R³B/LAND setup with incident beam energies in the range of 300–450 MeV/u. The oxygen isotopic chain offers a large variation of separation energies that allows for a quantitative understanding of single-particle strength with changing isospin asymmetry. Quasifree knockout reactions provide a complementary approach to intermediate-energy one-nucleon removal reactions. Inclusive cross sections for quasifree knockout reactions of the type ${}^A\text{O}(p, 2p){}^{A-1}\text{N}$ have been determined and compared to calculations based on the eikonal reaction theory. The reduction factors for the single-particle strength with respect to the independent-particle model were obtained and compared to state-of-the-art *ab initio* predictions. The results do not show any significant dependence on proton-neutron asymmetry.

DOI: 10.1103/PhysRevLett.120.052501

States near the Fermi surface of closed-shell nuclei display single-particle (SP) behavior [1,2]. This fact underpins the success of the nuclear shell model (SM) [3] and motivates a simplified description of nuclei in terms of an independent-particle model (IPM), in which nucleons move freely in an average potential. Deviations from the simple IPM description have been quantified by $(e, e'p)$ measurements on stable nuclei, for instance, at the NIKHEF facility, evidencing that the strength of dominant SP states, the so-called spectroscopic factor (SF), is reduced by about 30%–40% in comparison to predictions based on the IPM [4,5]. This deviation can be understood as a consequence of correlations among nucleons leading to a fragmentation of the SP strength and a partial occupation of states above the Fermi energy.

Correlations among the nucleons are taken into account in the SM, which reproduces the resulting configuration mixing and SP strength distribution close to the Fermi surface reasonably well. Still, an overall reduction of SFs compared to the SM has been reported, which is usually quantified by a reduction factor R , defined as the ratio of the experimental cross section to theoretical predictions (based on either the IPM or SM). These remaining deviations are often attributed to correlations beyond those taken into account in the SM such as short-range correlations (SRC), including those induced by the short-range tensor interaction [6–8]. We note that signatures of SRC in momentum distributions [9] and strong proton-neutron correlations [10,11] have been observed in high-energy electron scattering.

The first systematic studies on SFs for unstable isotopes have been undertaken by evaluating one-nucleon removal cross sections at intermediate energies close to 100 MeV/u

[12] [One-nucleon removal encompasses any process producing an $A-1$ nucleus in the final state including different reaction mechanisms such as individual nucleon-nucleon collisions or inelastic excitation and decay. Still, this process is sometimes referred to as (heavy-ion induced) knockout in the literature.]. A recent compilation of the existing data by Tostevin and Gade [13] reports reduction factors relative to the SM description for a large number of isotopes. While the residual interactions in SM calculations can account for the spread of the SP strength near the Fermi surface, the data of Ref. [13] suggest a very strong dependence of SFs on the isospin asymmetry of nuclei, quantified by the difference between one-proton and one-neutron separation energies $\pm(S_p - S_n)$. In contrast, more recent results from transfer reactions at lower beam energies suggest a constant quenching of SFs and do not indicate such a pronounced isospin dependence [14–16]. *Ab initio* calculations, such as the self-consistent Green's function (SCGF) [17,18] or coupled-cluster theory [19], suggest indeed a reduction of SFs due to correlations but with a weak asymmetry dependence.

The isospin dependence is still heavily debated and it is unsettled whether this is an indication of correlation effects missing in SM calculations [20] or deficiencies in the reaction model, which is based on the sudden and eikonal approximations [21]. In particular, an asymmetric momentum distribution with a very large tail towards low momenta was observed in Ref. [21] after removing a tightly bound nucleon, indicating strong deviations from the approximations made. An additional potential issue lies in the fact that the sensitivity of the one-nucleon removal reaction induced by light composite nuclear targets, e.g., Be or C, at intermediate beam energies of around 100 MeV/u is concentrated strongly at the nuclear surface [22,23], probing only the outer part of the projectile wave function, which limits the access to deeply bound states.

In this Letter, we introduce a complementary experimental approach based on quasifree scattering (QFS)

Published by the American Physical Society under the terms of the Creative Commons Attribution 4.0 International license. Further distribution of this work must maintain attribution to the author(s) and the published article's title, journal citation, and DOI.

reactions in inverse and complete kinematics using a proton target bombarded by a high-energy beam of radioactive and stable nuclei. The oxygen isotopic chain provides thereby a large selection of nuclei with different nucleon separation energies that are suitable for a systematic study of the asymmetry dependence of the SP strength.

The usage of proton targets increases the sensitivity to deeply bound states, which in turn allows for a more complete investigation of the SP wave function [24]. Since the nucleon-nucleon (NN) total cross section has a minimum at around 300 MeV, final-state interactions, such as rescattering and absorption effects, are minimized at beam energies of around 400 MeV/u, where the energies of the outgoing nucleons amount to 200 MeV on average. At these energies, the picture of a localized reaction is supported, which can be described as an elementary QFS process between the struck nucleon and the target proton, where both nucleons are scattered at large angles centered around 45° [25]. Below 100 MeV, the NN cross section rises steeply and causes a strong distortion of the outgoing nucleon wave functions; i.e., the nucleus becomes opaque and the reaction thus probes only the surface at lower beam energies.

The theoretical description of QFS used here is based on the eikonal reaction model where the effect of multiple scattering is treated by use of the distorted wave impulse approximation with a complex optical potential [24]. The internal momentum of the knocked-out nucleon is related directly to the recoil momentum of the residual fragment, which is measured experimentally, and can be interpreted in terms of the angular momentum of the corresponding SP state.

The experiment was performed at the R³B/LAND setup at GSI Helmholtzzentrum für Schwerionenforschung in Darmstadt, Germany. A primary ^{40}Ar beam was accelerated up to 500 MeV/u and directed onto a Be target. The heavy reaction fragments were selected in the fragment separator FRS according to their magnetic rigidity [26] and transported to the experimental hall. The secondary beam was delivered as a cocktail beam containing different isotopes around a certain nominal rigidity. The incoming ions were identified on an event-by-event basis. The solid reaction targets were located at the center of the Crystal Ball detector array (CB) [27] and surrounded by double-sided silicon strip detectors (DSSSD) [28] for energy-loss and position measurements. The CB covers a solid angle of close to 4π and was used for the detection of γ rays and high-energy nucleons from the knockout reactions. The heavy reaction products were deflected by the dipole magnet ALADIN and charges and masses were reconstructed by several tracking detectors. A detailed description of the setup can be found in Refs. [25,29–32]. The experiment was performed with CH_2 (458 and 922 mg/cm²) and C (558 and 935 mg/cm²) targets as well as with an empty target frame. The C target was used to estimate and subtract C-induced reactions in the CH_2 target, while measurements without target were made to estimate background contributions.

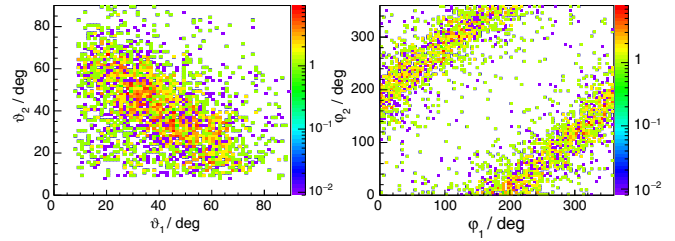


FIG. 1. Correlations of polar (θ) and azimuthal (ϕ) angles of two protons detected in the CB for the reaction $^{16}\text{O}(p, 2p)^{15}\text{N}$ measured in coincidence with the ^{15}N fragment.

The angular correlations of the knocked-out projectile nucleon and the recoiled target proton shown in Fig. 1 for the reaction $^{16}\text{O}(p, 2p)^{15}\text{N}$ exhibit the characteristics of QFS indicating a nearly coplanar back-to-back scattering. Slight modifications compared to free NN scattering are caused by the binding energy and the internal motion of the nucleons in the nucleus [25]. A coincident measurement of the knocked-out and recoiled nucleons as well as of the residual fragment allows an unambiguous and practically background-free reconstruction of QFS channels.

It is emphasized that all reaction channels were selected requiring the simultaneous detection of two protons and a bound residual N fragment ($A-1$) in the final state. The inclusive cross sections thus contain the population of the ground and bound excited states of the fragment. In order to extract the exclusive cross sections for the population of excited states below the particle threshold, the measurement of γ rays in coincidence has been analyzed for all reaction channels. In the following paragraphs, the reaction $^{16}\text{O}(p, 2p)^{15}\text{N}$ will be presented in detail and the results of the other reaction channels will be summarized later. Additional results including γ spectra and momentum distributions for the other isotopes will be presented together with a more detailed description of the analysis procedure in a forthcoming article.

The measured cross sections were subject to various corrections such as the $2p$ detection efficiency, which was crucial since its uncertainty dominates the systematic uncertainty of the deduced cross sections. This efficiency has been obtained from simulations of $(p, 2p)$ events according to the QFS kinematics at the various beam energies listed in Table I. The simulation of the experiment was performed within the R3BRoot framework [33,34] based on the GEANT4 toolkit [35] and using different physics models [36–38] for the treatment of reactions in the detector material. The observed 6% variation of the deduced detection efficiency of 63% with the different model inputs was treated as a systemic uncertainty. For the reaction $^{16}\text{O}(p, 2p)^{15}\text{N}$, for instance, an inclusive cross section of 26.8(9)[1.7] mb was deduced, where the systematic uncertainty is given in square brackets (see Table I). This cross section includes proton knockout from the $0p_{1/2}$ orbit to the ground state (g. s.) of ^{15}N and from the $0p_{3/2}$

TABLE I. Measured and calculated ($p, 2p$) cross sections for the reactions given in the first column. The second and third columns give neutron and proton separation energies of the residual $A-1$ N, respectively [39,40]. In the fourth column, the mean beam energy in the middle of the CH₂ target is given. In the fifth column, inclusive cross sections for all bound states are listed along with statistical (round brackets) and systematic uncertainties (square brackets). The predictions from eikonal theory (sixth column) are shown for the knockout of $0p_{1/2}$ protons except for ^{16}O , where the sum of $0p_{1/2}$ and $0p_{3/2}$ contributions is given. The last column gives the resulting reduction factor R relative to the IPM with its total uncertainty.

Reaction	$S_n(^{A-1}\text{N})$ [MeV]	$S_p(^{A-1}\text{N})$ [MeV]	E_{beam} [MeV/u]	σ_{exp} [mb]	σ_{theory} [mb]	R
$^{13}\text{O}(p, 2p)^{12}\text{N}$	15.0	0.60	401	5.78(0.91)[0.37]	18.96	...
$^{14}\text{O}(p, 2p)^{13}\text{N}$	20.1	1.94	351	10.23(0.80)[0.65]	15.09	0.68(7)
$^{15}\text{O}(p, 2p)^{14}\text{N}$	10.6	7.55	310	18.92(1.82)[1.20]	12.19	...
$^{16}\text{O}(p, 2p)^{15}\text{N}$	10.9	10.2	451	26.84(0.90)[1.70]	38.34	0.70(5)
$^{17}\text{O}(p, 2p)^{16}\text{N}$	2.49	11.5	406	7.90(0.26)[0.50]	12.23	0.65(5)
$^{18}\text{O}(p, 2p)^{17}\text{N}$	5.89	13.1	368	17.80(1.04)[1.13]	9.95	...
$^{21}\text{O}(p, 2p)^{20}\text{N}$	2.16	17.9	449	5.31(0.23)[0.34]	9.16	0.58(4)
$^{22}\text{O}(p, 2p)^{21}\text{N}$	4.59	19.6	415	5.93(0.39)[0.40]	8.54	...
$^{23}\text{O}(p, 2p)^{22}\text{N}$	1.28	21.2	448	5.01(0.97)[0.33]	8.06	0.62(13)

orbit to bound excited states (see discussion below). The removal of a proton from the $0s_{1/2}$ orbit can only populate unbound states of ^{15}N and is thus not considered.

Figure 2 shows the projection of the transverse momentum distribution of ^{15}N on the y axis (symbols). Since this includes proton knockout from the $0p_{1/2}$ and $0p_{3/2}$ orbits, it is compared to the sum of the theoretical distributions for both orbits. The theoretical cross sections were calculated with the eikonal theory of Ref. [24] and amount to 13.2 and 25.1 mb assuming knockout from completely filled $0p_{1/2}$ and $0p_{3/2}$ orbits, respectively. The reduction factor R amounts to $R = 0.70(5)$ and agrees well with the result $R = 0.65(5)$ from ($e, e'p$) data [5]. The dash-dotted curve in Fig. 2 shows the distribution of the total spectrum (solid) scaled by R . The scaled distribution describes the

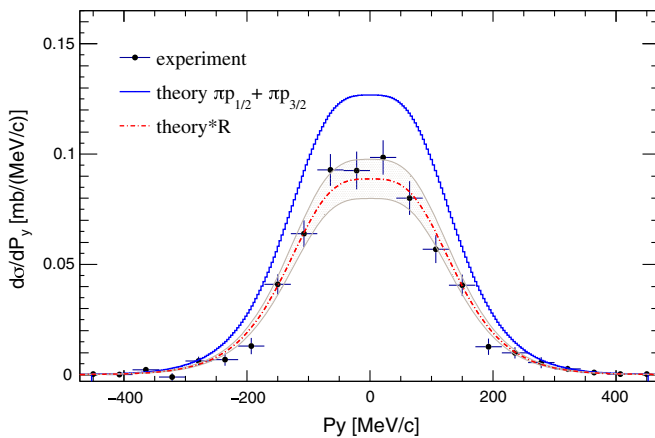


FIG. 2. Projection P_y of the momentum distribution of ^{15}N after one-proton removal from ^{16}O , compared to the sum of theoretical distributions for the $0p_{1/2}$ and $0p_{3/2}$ orbits (solid curve) and the one scaled to the experimental cross section (dashed-dotted curve with shaded 2σ uncertainty range).

experimental data well, confirming our assumption that the data is dominated by proton knockout from orbits of $\ell = 1$.

Exclusive cross sections were extracted from a fit to the coincident γ spectrum as shown in Fig. 3 for the $^{16}\text{O}(p, 2p)^{15}\text{N}$ reaction. Besides the simulated two transitions from the excited $3/2^-$ states at 6.63 and 9.93 MeV, a background contribution arising from ($p, 2p$) reactions without γ -ray emission was included in the fit. The population of the g. s. was obtained by subtracting the contribution of the excited states from the total cross section resulting in SF values of 1.60(39), 2.01(23), and 0.58(13) for populating the g. s. and the $3/2^-$ states at 6.63 and 9.93 MeV, respectively. Note that the measured SF for the $1/2^-$ g. s. amounts to 80% of the IPM, while the $0p_{3/2}$ strength adds up to 65%, whereas the SCGF calculation discussed below predicts 78% and 80%, respectively. However, theory does not reproduce the observed

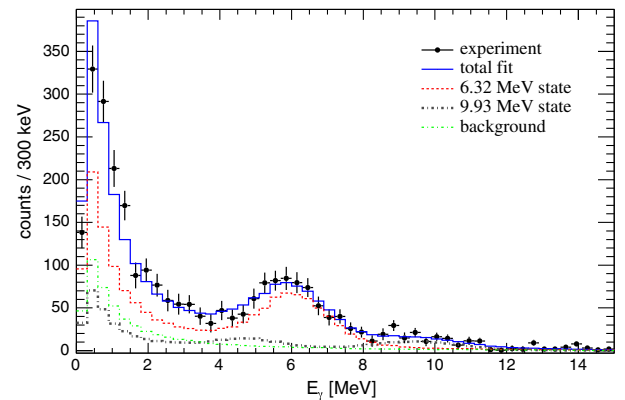


FIG. 3. Doppler-corrected single- γ spectrum measured in coincidence with ^{15}N and two protons in CB. The simulated decays of the $3/2^-$ states at 6.32 and 9.93 MeV were fitted to the experimental data together with the background contribution. The total fit is displayed by the solid curve.

fragmentation of $3/2^-$ strength, which is collected in one single state. The experimental SF values for the states discussed above are consistent with the results from $(e, e'p)$ data [41,42].

The measured inclusive cross sections for proton knockout are listed in Table I. Since only bound states of the residual $A-1N$ are detected, the results fluctuate with changes of the separation energies along the isotopic chain as a consequence of the very different nucleon separation energies of the daughter nuclei. $^{16}\text{O}(p, 2p)^{15}\text{N}$ has the largest cross section since both knockout from $0p_{1/2}$ and $0p_{3/2}$ populate bound states in ^{15}N . For the $^{15}\text{O}(p, 2p)^{14}\text{N}$ and $^{18}\text{O}(p, 2p)^{17}\text{N}$ reactions, the $0p_{1/2}$ protons contribute fully, but only part of the (fragmented) $0p_{3/2}$ strength is below the continuum threshold. The case is similar for the ^{22}O projectile, albeit with a larger contribution of the $0p_{3/2}$ proton strength due to the relatively large neutron separation energy of 4.59 MeV of the daughter nucleus ^{21}N [39]. The case of $^{13}\text{O}(p, 2p)^{12}\text{N}$ is at the other extreme, since the knockout from the $0p_{1/2}$ orbit contributes only partially to the cross section due to the very weakly bound protons in ^{12}N ($S_p = 0.6$ MeV [39]). The rest of the reaction channels can be safely considered as arising from the full $0p_{1/2}$ proton knockout alone. Table I also gives the corresponding theoretical cross sections, assuming the IPM occupation.

For the discussion of the reduction factor R , we concentrate on the aforementioned isotopes, where it is reasonable to assume that the full $0p_{1/2}$ strength is collected in bound states, while the $0p_{3/2}$ strength is exclusively located in the continuum. We also include the one exception for ^{16}O , where also the $0p_{3/2}$ hole states are bound. We exclude cases where the $0p_{3/2}$ strength is located close to the particle separation threshold and is fragmented. Such a selection is possible since the structure of the produced nuclei is known and, in addition, the γ spectra of the final states were analyzed. For the selected cases, we can then compare the measured cross sections directly to the theoretical ones based on the IPM without the need for additional theoretical structure input, which would complicate the discussion on the asymmetry dependence.

The resulting R values are summarized in the last column of Table I and are displayed in Fig. 4 as a function of the difference of g. s. separation energies ($S_p - S_n$) as filled circles and as a square for ^{16}O , where the sum of $0p_{1/2}$ and $0p_{3/2}$ contributions is shown as discussed above. The error bars represent the statistical uncertainty while the horizontal square brackets indicate the total uncertainty including the systematic errors. This allows a direct comparison of R relative to each other without identical systematic uncertainties. The data from this work show a fluctuation of R around 0.66. The solid and dotted lines display fits with a linear function and with a constant value resulting in a reduced χ^2 of 1.29 and 1.91, respectively. We conclude that

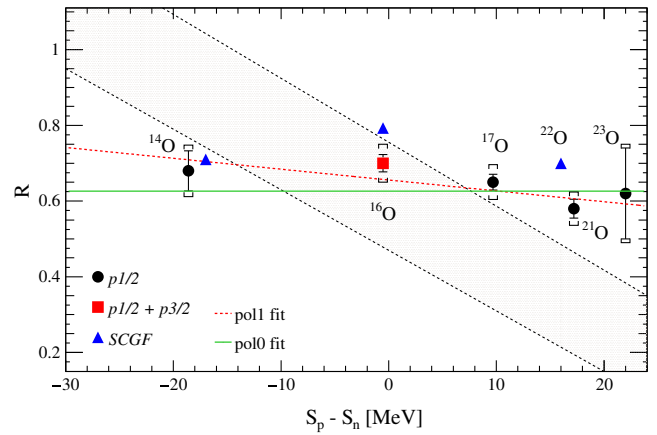


FIG. 4. Reduction factor R deduced from $(p, 2p)$ cross sections (circles and square) as a function of $S_p - S_n$ compared to theoretical SFs calculated with SCGF (triangles). The shaded area indicates the trend from an analysis of intermediate-energy one-nucleon removal cross sections.

the data are consistent with weak or even no dependence of the SP strength on the neutron-proton asymmetry. This trend differs drastically from the result of one-nucleon removal reactions at intermediate energies as compiled in Ref. [13]. Note that R is the ratio of the experimental cross section to the theoretical one based on the IPM, while the R values of Ref. [13] are given relative to a particular SM calculation. For the cases selected here, however, the fragmentation is small and the sum of the SM SF values reflects the sum-rule value given by the IPM. We estimated the uncertainties of the calculated cross sections related to possible variations of the input parameters within a reasonable range (NN cross sections, densities, and SP wave functions) to be less than 5%, i.e., significantly smaller than the experimental uncertainties. Our conclusion agrees with Ref. [16], where transfer data on ^{14}O have been analyzed. We note that our deduced reduction factor of 0.68(7) is in very good agreement with the one of 0.73(10)(10), derived from the $^{14}\text{O}(d, ^3\text{He})$ transfer [16].

Furthermore, we have performed state-of-the-art *ab initio* calculations of the proton-hole strength in $^{14,16,22}\text{O}$ based on the SCGF theory, using the third-order algebraic diagrammatic construction approach [ADC(3)] [18,43]. This is the method of choice for calculating the nuclear spectral function and yields the most accurate SF results near subshell closures. The theoretical SF can be sensitive to particle-hole gaps and the density of states at the Fermi surface [44]. Hence, we based our calculations on the saturating chiral interaction NNLO-sat [45], which guarantees the best possible predictions of radii and gaps in this region of the nuclear chart [46]. The resulting SF values shown as blue triangles in Fig. 4 for proton removal to the ground states of ^{13}N and ^{21}N and for summed p -shell states in ^{15}N are in reasonable agreement with the present measurements, although they seem to overestimate the

$3/2^-$ strength in ^{15}N , where theory does not reproduce the correct fragmentation as explained above. These results are also compatible with earlier microscopic studies [47] as well as $(e, e'p)$ data [5]. As was seen for other nuclear interactions [17,18], the SF from NNLO-sat depend little on isospin asymmetry. Note that continuum effects can further affect the quenching of SP strength in ^{22}O but not to the extent of altering this trend [19]. Thus, *ab initio* results do not support a significant dependence on isospin asymmetry, in agreement with the experimental results presented in this Letter.

In summary, we have measured inclusive $(p, 2p)$ cross sections for stable and unstable oxygen isotopes using the quasifree scattering technique in inverse kinematics and extracted the single-particle reduction factor R from the comparison with eikonal theory. The reduction obtained from the reaction $^{16}\text{O}(p, 2p)^{15}\text{N}$ shows good agreement with the results obtained from $(e, e'p)$ measurements. The results for stable and exotic nuclei indicate a weak or even no dependence on the proton-neutron asymmetry. This finding is compatible with the *ab initio* Green's function and coupled cluster calculations but contradicts the trend derived from intermediate-energy one-nucleon removal cross section measurements. This disagreement calls for further investigations of the reaction mechanism of nucleon removal from deeply bound states at intermediate energies. In the future, quasifree knockout reactions in inverse kinematics will allow for a systematic investigation of proton and neutron knockout from exotic nuclei covering a wide range of neutron-to-proton asymmetry, which will be important to corroborate the observed trend and to improve our understanding on the evolution of the single-particle structure as a function of neutron-to-proton asymmetry.

This work was supported by the German Federal Ministry for Education and Research (BMBF project 05P15RDFN1), and through the GSI-TU Darmstadt cooperation agreement. The work of C. B., W. C., and G. W. was supported by the United Kingdom Science and Technology Facilities Council (STFC) under Grants No. ST/L005743/1 and No. ST/P005314/1. SCGF calculations were performed at the DiRAC Complexity system of the University of Leicester (BIS National E-1023 infrastructure capital Grant No. ST/K000373/1 and STFC 1024 Grant No. ST/K0003259/1). C. A. B. acknowledges support by the U.S. DOE Grant No. DE-FG02-08ER41533 and the U.S. NSF Grant No. 1415656. L. M. F. acknowledges funding from MINECO FPA2015-65035-P project.

*L.Atar@gsi.de

Present address: Department of Physics, University of Guelph, Guelph, Ontario N1G 2W1, Canada.

†t.aumann@gsi.de

[1] M. G. Mayer, *Phys. Rev.* **75**, 1969 (1949).

- [2] O. Haxel, J. H. D. Jensen, and H. E. Suess, *Phys. Rev.* **75**, 1766 (1949).
- [3] E. Caurier, G. Martínez-Pinedo, F. Nowacki, A. Poves, and A. P. Zuker, *Rev. Mod. Phys.* **77**, 427 (2005).
- [4] I. Sick, *Prog. Part. Nucl. Phys.* **59**, 447 (2007).
- [5] L. Lapikás, *Nucl. Phys.* **A553**, 297 (1993).
- [6] C. Barbieri, *Phys. Rev. Lett.* **103**, 202502 (2009).
- [7] W. Dickhoff and C. Barbieri, *Prog. Part. Nucl. Phys.* **52**, 377 (2004).
- [8] V. R. Pandharipande, I. Sick, and P. K. A. d. Huberts, *Rev. Mod. Phys.* **69**, 981 (1997).
- [9] D. Rohe *et al.* (E97-006 Collaboration), *Phys. Rev. Lett.* **93**, 182501 (2004).
- [10] R. Subedi *et al.*, *Science* **320**, 1476 (2008).
- [11] O. Hen *et al.* (J. L. C. Collaboration), *Science* **346**, 614 (2014).
- [12] P. G. Hansen and J. A. Tostevin, *Annu. Rev. Nucl. Part. Sci.* **53**, 219 (2003).
- [13] J. A. Tostevin and A. Gade, *Phys. Rev. C* **90**, 057602 (2014).
- [14] J. Lee *et al.*, *Phys. Rev. Lett.* **104**, 112701 (2010).
- [15] B. P. Kay, J. P. Schiffer, and S. J. Freeman, *Phys. Rev. Lett.* **111**, 042502 (2013).
- [16] F. Flavigny *et al.*, *Phys. Rev. Lett.* **110**, 122503 (2013).
- [17] C. Barbieri and W. H. Dickhoff, *Int. J. Mod. Phys. A* **24**, 2060 (2009).
- [18] A. Cipollone, C. Barbieri, and P. Navrátil, *Phys. Rev. C* **92**, 014306 (2015).
- [19] O. Jensen, G. Hagen, M. Hjorth-Jensen, B. A. Brown, and A. Gade, *Phys. Rev. Lett.* **107**, 032501 (2011).
- [20] N. K. Timofeyuk, *Phys. Rev. C* **88**, 044315 (2013).
- [21] F. Flavigny, A. Obertelli, A. Bonaccorso, G. F. Grinyer, C. Louchart, L. Nalpas, and A. Signoracci, *Phys. Rev. Lett.* **108**, 252501 (2012).
- [22] A. Gade and T. Glasmacher, *Prog. Part. Nucl. Phys.* **60**, 161 (2008).
- [23] C. Bertulani and A. Gade, *Comput. Phys. Commun.* **175**, 372 (2006).
- [24] T. Aumann, C. A. Bertulani, and J. Ryckebusch, *Phys. Rev. C* **88**, 064610 (2013).
- [25] V. Panin *et al.*, *Phys. Lett. B* **753**, 204 (2016).
- [26] H. Geissel *et al.*, *Nucl. Instrum. Methods Phys. Res., Sect. B* **70**, 286 (1992).
- [27] V. Metag *et al.*, *Nucl. Phys.* **A409**, 331 (1983).
- [28] J. Alcaraz *et al.*, *Nucl. Instrum. Methods Phys. Res., Sect. A* **593**, 376 (2008).
- [29] C. Caesar *et al.* (R3B Collaboration), *Phys. Rev. C* **88**, 034313 (2013).
- [30] M. Röder *et al.* (R3B Collaboration), *Phys. Rev. C* **93**, 065807 (2016).
- [31] R. Thies *et al.* (R3B Collaboration), *Phys. Rev. C* **93**, 054601 (2016).
- [32] M. Heine *et al.* (R3B Collaboration), *Phys. Rev. C* **95**, 014613 (2017).
- [33] D. Bertini, *J. Phys. Conf. Ser.* **331**, 032036 (2011).
- [34] <http://fairroot.gsi.de>, accessed: 16.08. 2016.
- [35] S. Agostinelli, *Nucl. Instrum. Methods Phys. Res., Sect. A* **506**, 250 (2003).
- [36] J. Apostolakis, G. Folger, V. Grichine, A. Heikkinen, A. Howard, V. Ivanchenko, P. Kaitaniemi, T. Koi, M. Kosov,

- J. M. Quesada, A. Ribon, V. Uzhinskiy, and D. Wright, *J. Phys. Conf. Ser.* **160**, 012073 (2009).
- [37] D. Mancusi, A. Boudard, J. Cugnon, J.-C. David, P. Kaitaniemi, and S. Leray, *Phys. Rev. C* **90**, 054602 (2014).
- [38] D. H. Wright and M. H. Kelsey, *Nucl. Instrum. Methods Phys. Res., Sect. A* **804**, 175 (2015).
- [39] B. Pritychenko, E. Běták, M. Kellett, B. Singh, and J. Totans, *Nucl. Instrum. Methods Phys. Res., Sect. A* **640**, 213 (2011).
- [40] D. Sohler *et al.*, *Phys. Rev. C* **77**, 044303 (2008).
- [41] M. Leuschner, J. R. Calarco, F. W. Hersman, E. Jans, G. J. Kramer, L. Lapikás, G. van der Steenhoven, P. K. A. de Witt Huberts, H. P. Blok, N. Kalantar-Nayestanaki, and J. Friedrich, *Phys. Rev. C* **49**, 955 (1994).
- [42] M. Bernheim, A. Bussiere, J. Mougey, D. Royer, D. Tarnowski *et al.*, *Nucl. Phys.* **A375**, 381 (1982).
- [43] C. Barbieri and A. Carbone, *Lect. Notes Phys.* **936**, 571 (2017).
- [44] C. Barbieri and M. Hjorth-Jensen, *Phys. Rev. C* **79**, 064313 (2009).
- [45] A. Ekström, G. R. Jansen, K. A. Wendt, G. Hagen, T. Papenbrock, B. D. Carlsson, C. Forssén, M. Hjorth-Jensen, P. Navrátil, and W. Nazarewicz, *Phys. Rev. C* **91**, 051301 (2015).
- [46] V. Lapoux, V. Somà, C. Barbieri, H. Hergert, J. D. Holt, and S. R. Stroberg, *Phys. Rev. Lett.* **117**, 052501 (2016).
- [47] C. Barbieri and W. H. Dickhoff, *Phys. Rev. C* **65**, 064313 (2002).